



Article

Behavior of Sludge Dewaterability and Nutrient Contents after Treatment with Cellulose-Based Flocculants with Combined PTS and Catalytic Behavior of Sludge towards Tetracycline Degradation

Jannatul Rumky * , Ekaterina Bandina and Eveliina Repo

Department of Separation Science, LUT University, Sammonkatu 12, FI-50130 Mikkeli, Finland

* Correspondence: jannatul.rumky@lut.fi

Abstract: Wastewater treatment plants are increasingly interested in adopting inorganic coagulants and organic flocculants in their sludge treatment process since sludge disposal costs more than half of the overall operational costs. This study synthesized poly titanium sulfate (PTS) by different molar ratios and used the best one with cellulose-based flocculants for sludge conditioning. PTS synthesized with a 1:2 molar ratio showed the lowest capillary suction time (CST) of sludge and was selected for further studies with cellulose-based flocculants. As bio-based flocculants have gained popularity due to current environmental problems, cationized cellulose-based flocculants (Ce-CTA) were used in this work with or without PTS for sludge treatment. After coagulation–flocculation, dewaterability of sludge enhanced, and the Lowry and Anthrone method was used to assess proteins and polysaccharides. Next, metal content and nutrients such as total phosphorus, phosphate, and nitrate were measured by ICP-OES and IC, and we found promising results of phosphate especially at pH 3. Higher total phosphorus content was found at pH 3 and 9, and even at pH 6 after PTS or PTS+Ce-CTA treatment. In addition, PTS-treated sludge materials also showed catalytic behavior, suggesting a new research avenue for future development. Based on this study, the PTS+Ce-CTA combination is promising for sludge treatment and nutrient recovery, along with the possibility for the further valorization of the sludge materials.

Keywords: poly titanium sulfate; cellulose-based flocculants; coagulation; flocculation; dewaterability; phosphate; nitrate; heavy metals



Citation: Rumky, J.; Bandina, E.; Repo, E. Behavior of Sludge Dewaterability and Nutrient Contents after Treatment with Cellulose-Based Flocculants with Combined PTS and Catalytic Behavior of Sludge towards Tetracycline Degradation. *Resources* **2023**, *12*, 17. <https://doi.org/10.3390/resources12020017>

Academic Editor: Benjamin McLellan

Received: 7 September 2022

Revised: 15 December 2022

Accepted: 4 January 2023

Published: 17 January 2023



Copyright: © 2023 by the authors. Licensee MDPI, Basel, Switzerland. This article is an open access article distributed under the terms and conditions of the Creative Commons Attribution (CC BY) license (<https://creativecommons.org/licenses/by/4.0/>).

1. Introduction

The traditional activated sludge process of municipal wastewater produces a substantial amount of waste activated sludge (WAS), which is regarded as a carbon- and nutrient-rich end product. Anaerobic digestion is now mostly utilized to stabilize the WAS, giving benefits such as biogas production, pathogen removal, and odor reduction. However, sustainable management of anaerobically digested sludge (ADS) is one of the most pressing concerns in wastewater treatment facilities due to the complex physicochemical characteristics of ADS, the expenses involved with sludge dewatering, and stringent environmental regulations for final disposal [1,2]. ADS is a water- and nutrient-rich sludge in which water is attached to the solid particles and cannot be effectively removed using conventional physical processes, such as press filtration or centrifugation, which leads to significant drying costs. In addition, extracellular polymeric substances (EPS), which consist of several high molecular weight biopolymers, allow water molecules to be entrapped and effect sludge dewaterability [3,4].

It has been demonstrated that high-performance dewatering is an effective way for reducing sludge volume, hence reducing transportation and disposal costs. Preconditioning using an inorganic coagulant (Fe or Al salt) or a synthetic polyelectrolyte such as

polyacrylamide, followed by centrifugation or pressing, is the typical method for sludge dewatering [5]. Aside from sludge properties, the dewatering efficiency mostly depends on the type of solid–liquid separation equipment and sludge pre-conditioning techniques. Researchers have thus evaluated numerous preconditioning approaches, such as ultrasonic conditioning [6], advanced oxidation [7,8], thermal treatment, freezing and thawing, addition of porous materials, or the addition of chemicals including acids, bases, surfactants, oxidants and skeleton builders [9]. However, coagulant–flocculant-based sludge preconditioning is one of the most extensively utilized approaches in terms of costs and efficiency in large scale applications. In the coagulation–flocculation process, small colloidal particles in the sludge form large flocs by neutralizing their charges and creating a path for smaller particles to cross from one side of the sludge to the other, increasing sedimentation and dewatering output and reducing the sludge settling time [10–12].

Due to their low cost, aluminum and iron salts are extensively utilized as coagulants. However, Al/Fe coagulants have several downsides, such as small floc size, long sedimentation duration, and creation of unpleasant color and odor in the effluent. A non-toxic and efficient alternative for Al/Fe coagulants is titanium salt-based coagulant, which provides coagulated effluents with lower metal concentrations [13]. However, a significant knowledge gap exists in the application of Ti-based coagulants for sludge dewatering [14]. In addition, during high temperature pyrolysis, residuals from titanium salt coagulation may be transformed into carbon-supported TiO₂ materials [15,16]. Moreover, complete hydrolysis and the low solubility of the formed Ti(OH)₄ and, the concentration levels of residual metals in the Ti coagulated effluents are generally much lower than those of Al/Fe coagulants. After Al/Fe coagulant treatment, researchers try to recover or use them in construction materials, but PTS-treated sludge might be developed as a photocatalyst and degrade other pollutants from wastewater under UV, visible light, etc.

In addition to inorganic coagulants, organic polymeric flocculant methods are now being practiced as new sludge preconditioning techniques. Polysaccharide-based flocculants are favored because they are both affordable and environmentally friendly. Some physical/chemical modifications, such as etherification and graft polymerization, can also improve flocculation performance [17,18]. Cellulose, a polymer made of long chains of polysaccharides, shows potential as a flocculant due to its biodegradable properties and its repeated blocks of D-glucose. Cellulose is obtainable from various sources such as cotton fibers, wood fibers, bamboo, grass, algae, and bacteria. Furthermore, it has better water purification qualities due to the presence of free -OH groups on the chain, enabling it to remove organic matter and metal ions efficiently. Additionally, cellulose reactivity can be increased, for example by alkalization with NaOH or cationization with CHPTAC (3-chloro-2-hydroxypropyl trimethylammonium chloride) [19].

In addition to dewatering performance, the behavior of heavy metals and other resources (e.g., phosphorus) after coagulation–flocculation have become an important aspect. Ida and Eva [20] identified coagulation–flocculation as one of the most promising methods for heavy metal recovery during or right after primary settling though it had less impact on Ni removal. In addition, both inorganic and organic forms of phosphorus can be found in water. Different treatment techniques (crystallization, precipitation, ion exchange, etc.) have been used for inorganic phosphorus removal [21–23] but traditional techniques are not well-suited for organic phosphates due to their unique structures. Natural polymers for phosphorus removal have not been extensively studied, but it was shown that adding a starch-based flocculant with FeCl₃ may save one-third of the total cost of pre-treatment while 90% of total phosphorus was reduced [22,24].

So far, no research has been reported on the treatment of ADS using poly titanium sulfate coagulants and cellulose-based polymeric flocculants. Therefore, in this study (Figure 1), poly titanium sulfate coagulants and cellulose-based flocculants were synthesized and used for the treatment of digested sludge. Efficiency of the treatment was verified by determining SVI and dewaterability and analyzing nutrient and metal concentrations in the supernatant. Finally, Ti-coagulated residual material was pyrolyzed and investigated

for tetracycline removal under UV radiation to check the photocatalytic activity at different pH ranges.

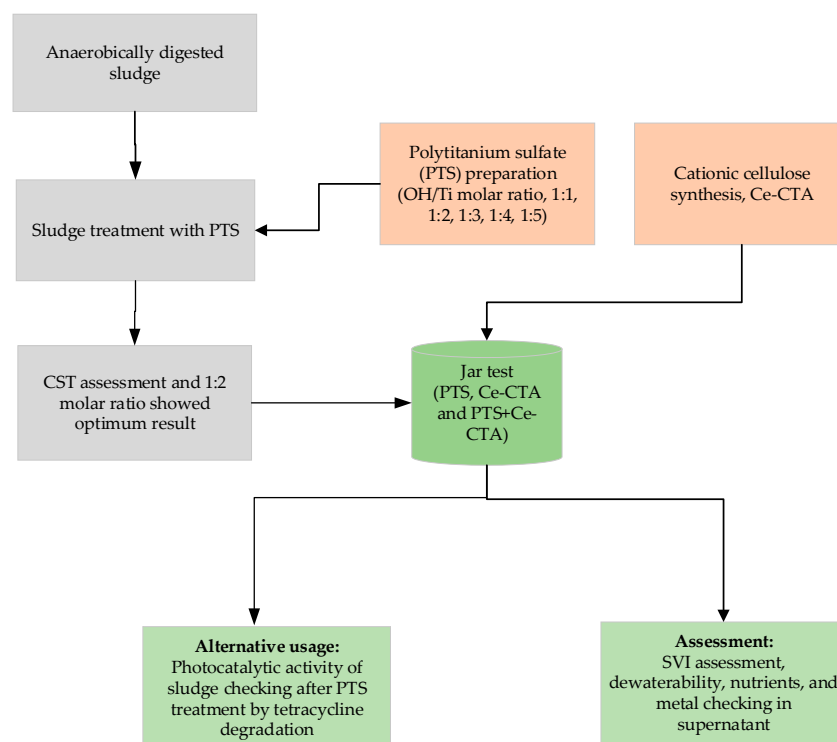


Figure 1. Flow chart of coagulation–flocculation treatment of sludge materials.

2. Materials and Methods

2.1. Materials

Cellulose (microcrystalline powder) was obtained from Merck (Sigma Aldrich, St. Louis, MO, USA), and 3-chloro-2-hydroxypropyl trimethyl ammonium chloride (CTA, with 65 wt% in water, Sigma Aldrich), ethanol (ETAX AA, 99.5%, ALTIA Oyj, Helsinki, Finland), and acetone (Sigma Aldrich) were used for cellulose modification. Sodium hydroxide and hydrochloric acid were of analytical grade and purchased from Sigma Aldrich and used to control pH. Titanium sulfate (Fisher Scientific, Waltham, MA, USA) was used for poly titanium sulfate preparation. Oxytetracycline hydrochloride (Merck, Sigma Aldrich) was used in degradation studies to assess photocatalytic activity of sludge.

Anaerobically digested sludge was collected from the local WWTP, Mikkeli, Finland, and after collection, sludge samples were stored at 4 °C for less than five days before processing to keep their properties unaltered.

2.2. Cationic Cellulose and Poly Titanium Sulfate Preparation and Characterization

Cationic cellulose (Cat-Ce) was obtained by etherification through the same procedure described by Wei et al., 2018 for starch-based flocculant. CTA was considered as the etherifying agent and cationic cellulose prepared by adding 1:1 mass ratio of cellulose: CTA. The molecular structures of the Cat-Ce sample were characterized using Fourier transform infrared spectroscopy (FTIR, Perkin Elmer Frontier ATR module) and the FTIR spectra are depicted in supporting information Figure S1a.

Poly titanium sulfate (PTS) was made by slowly adding 200.0 g/L NaOH solution (pre-determined amount, flow rate of 0.5 mL/min) into titanium sulfate solution (15% solution, $\rho = 1.36$ g/mL, Fisher Scientific). A magnetic stirrer was used to maintain a mixing speed of 700–800 rpm. During the process, the following OH/Ti molar ratio values were chosen: 1:1, 1:2, 1:3, 1:4, and 1:5 and the resultant samples were designated as PTS01, PTS02, PTS03, PTS04, and PTS05.

2.3. Sludge Conditioning

Sludge samples (500 mL) were conditioned with coagulants–flocculants using a program-controlled paddle apparatus (Stuart, SW6, Cole-Parmer Ltd., Vernon Hills, IL, USA) with six beakers. Conditioning was done by 1% dosage of coagulant–flocculant as follows: rapid mixing at 250 rpm for 2 min, followed by slow mixing at 50 rpm for 5 min for each conditioner (this procedure would be conducted twice if two conditioners were used successively), and 30 min of standing time. Finally, the methods described below were used to measure the sludge volume index (SVI), heavy metals, nutrients, and EPS characteristics.

2.4. Sludge Volume Index (SVI)

Sludge Volume Index (SVI) was calculated to measure settleability after coagulation. This test followed the standard procedures [25]. An Imhoff 1 L graduated cylinder was used for the SVI sludge settling test. The best treatment efficiencies were defined based on the SVI tests. A 30 min settling time was used to measure the settled sludge volume after adding a coagulant to a jar test setup and the settled sludge volume was also monitored after 60 min.

2.5. CST Measurement of Sludge after PTS Treatment

The capillary suction time (CST) test is a commonly used method to measure the filterability and the easiness of removing moisture from slurry and sludge in numerous environmental and industrial applications. Here, the CST of sludge was analyzed by CST 304 M to check sludge filterability after coagulation–flocculation.

2.6. EPS Extraction

Refined extraction methods were used to extract the two types of polymers (TB-EPS and LB-EPS) found in the sludge materials. Sludge samples were first centrifuged at 4 °C and $4000 \times g$ for 10 min and then vortexed with 0.5% NaCl and centrifuged again. Samples were sonicated (3–4 min), and sonicated samples then centrifuged again at $4000 \times g$ for 12 min. The supernatant was filtered through a 0.45 μm polypropylene (PP) filter, and TB-EPS analyzed. 0.05% NaCl was added to the corresponding solution using vortex and held at 60 °C for 30 min. In the final step, the supernatant was passed through the 0.45 μm PP filter and TB-EPS measured. Polysaccharides and proteins are present in every sample fraction [26,27]. We used the Lowry method to analyze proteins in bovine serum albumin. Polysaccharide levels were measured using glucose as a reference standard using the Anthrone method [28]. For greater precision, each experiment was conducted three times.

2.7. Heavy Metal and Phosphorus Assessment

Three different pH controlled tests were used here as it is proven by different researchers that high phosphate release is observed mainly at acidic and alkaline pH [29]. So, a total of ten samples were taken for the analysis and pH 3, 6, and 9 were maintained for PTS and Ce-CTA treatment. PTS, Ce-CTA, and PTS+Ce-CTA treatments were conducted and samples regarded as sample-1 (pH-3, PTS treatment), sample-2 (pH-3, Ce-CTA treatment), sample-3 (pH 3, PTS+Ce-CTA), sample-4 (pH-6, PTS treatment), sample-5 (pH-6, Ce-CTA treatment), sample-6 (pH 6, PTS+Ce-CTA), sample-7 (pH-9, PTS treatment), sample-8 (pH-9, Ce-CTA treatment), and sample-9 (pH 9, PTS+Ce-CTA). The presence of Cu, Ni, Pb, Cr, Zn, and P was analyzed by an inductively coupled plasma optical emission spectrometer (Agilent Technologies ICP-OES 5110). Phosphate concentration was also analyzed by ion chromatography (Schimadzu, Shodex IC SI-50 4E) from the supernatant.

2.8. Sludge Pyrolysis and Photocatalytic Activity Assessment

For photocatalytic activity testing, the sludge sample after PTS treatment was dried in an oven at 105 °C for 12 h, and then the unmodified sludge samples were recorded as sludge raw. A tube furnace (Carbolite Gero 30–3000 °C) with a N_2 atmosphere was

used to pyrolyze the modified sludge samples for an hour at 300 °C. By maintaining a heating rate of 5 °C/min, this pyrolyzed sludge sample was allowed to be cooled to room temperature naturally.

A certain amount of dried sludge (after PTS treatment) and pyrolyzed sludge photocatalyst was assessed by a certain concentration of tetracycline solution (1 g/L) and stirred under UV for 4 h to ensure the full tetracycline degradation. The clear liquid was analyzed by a spectrophotometer at time intervals to check the photocatalytic efficiency of dried and pyrolyzed sludge. In order to eliminate the effect of temperature on the experiment, the reaction temperature was maintained at 25 °C.

2.9. XRD and FTIR Analysis

In order to recognize the materials available in sludge, XRD and FTIR were used. XRD analysis was conducted with a Bruker D8 Advance diffractometer with Cu K α irradiation and FTIR with a Perkin Elmer Frontier with a universal ATR module (Diamond crystal).

3. Results and Discussion

3.1. Sludge Treatment with PTS and Ce-CTA

Sludge was assessed with different molar ratios of PTS (PTS 01 to PTS 05) and the capillary suction time (CST) of sludge was investigated to check the best PTS coagulant for further treatment with synthesized Ce-CTA.

A 1:2 molar ratio of PTS (as PTS 02) was proven to be the most effective coagulant for sludge treatment at neutral pH and selected for further treatment with Ce-CTA. PTS02 treated sludge's CST decreased a maximum 30–35%, which is a promising result for filterability and dewaterability enhancement of sludge. The zeta potential has also scientifically proven that for floc formation, cationic coagulants are more promising for anionic sludge (zeta potential of sludge in range -8 to -12 mV) [30]. From the synthesized different molar ratios of PTS, only PTS02 showed a cationic zeta potential ($+1.48$ mV). We can see PTS02 showed better performance (by considering CST) than PTS03 or PTS04. These results agreed with Huang et al. [31] and zeta potential decreased here in accordance with a higher OH/Ti molar ratio and all were below -13 mV.

Further, PTS02 and Ce-CTA were evaluated in the jar test and SVI were measured to analyze the settleability rate of sludge materials after jar tests. SVI is a critical variable in the sedimentation of particulate matter, and it denotes a volume (in milliliters) occupied by a gram of sludge after 30 min of settling. PTS, Ce-CTA, and PTS+Ce-CTA showed SVI values of 23.5, 55.5, and 20.7 mL/g, respectively, for sludge samples with neutral pH. Sludge that has a high SVI indicates that it has a low tendency to settle under gravity. As a result, in the settleability test, the sludge compacts poorly and settles slowly at high SVI. Difficulty in faster settlement is usually indicated by an SVI at nearly 80 [32]. SVI is calculated based on the below equation:

$$\text{SVI} \frac{\text{mL}}{\text{g}} = \frac{\text{Settled sludge volume mL/L}}{\text{Suspended solid concentration mg/L}} * \frac{100\text{mg}}{\text{g}} \quad (1)$$

Moreover, FTIR and XRD were used to characterize the sludge materials after treatment along with synthesized PTS and Ce-CTA. The synthesized PTS (at different ratios) did not show any significant changes according to Figures S1 and S2, so capillary suction time from sludge materials was measured; further, PTS02 was considered to be used with Ce-CTA as it showed best CST value. The peak at 3454.51 cm^{-1} relates to the stretching and the adsorption band at 1631.78 cm^{-1} represents the bending vibration of O-H, which defines the moisture. The intense peak at 690.52 cm^{-1} is assigned to the Ti-O stretching which is the characteristic peak of TiO. Additionally, the peak at 1085 cm^{-1} corresponding to anhydrous sulfate salt or sodium sulphate can be observed [33,34]. The cellulose-based material (Ce-CTA) also showed a broad band at 3448 cm^{-1} that is attributed to the stretching of the hydroxyl groups (Figure S3). CH₃ stretching could be observed at 2950 cm^{-1} and the vibrations of -CH₂- group at 1062 cm^{-1} . Moreover, the peak at 1414 cm^{-1} referring to

C-N stretching vibration verified the introduction of the quaternary ammonium salt group on the cellulose backbone. In addition, the presence of absorbed cellulose water gave a signal of the H–O–H bending group at 1674 cm^{-1} and C=C bonds created small peaks at $995\text{--}985$ [35,36].

Raw sludge, PTS treated, and PTS+Ce-CTA treated sludge samples are shown in XRD data in Figures S4–S6. From the XRD data of sludge, we found whitlockite, SiO_2 , Al_2O_3 , FeCO_3 , and vivianite. Later after treatment, silica, iron materials, and pyracmonite $(\text{NH}_4)_3\text{Fe}(\text{SO}_4)_3$ were also found.

The SEM images of sludge materials before and after coagulation–flocculation are presented in Figure 2. Figure 2a–c represents the digested sludge appearance as larger particles that are rough and have pores. The surface flatness could be noticed after coagulation–flocculation and Figure 2f,g also shows a visible surface area increasement. Figure 2k,l, on the other hand, illustrates a block-like structure and pores after PTS+Ce-CTA treatment. A typical particle's physical shape is depicted in SEM pictures. Due to colloidal particles contained in these flocs, the flocs formed following the coagulation–flocculation process were compact and had smooth surface morphology [37].

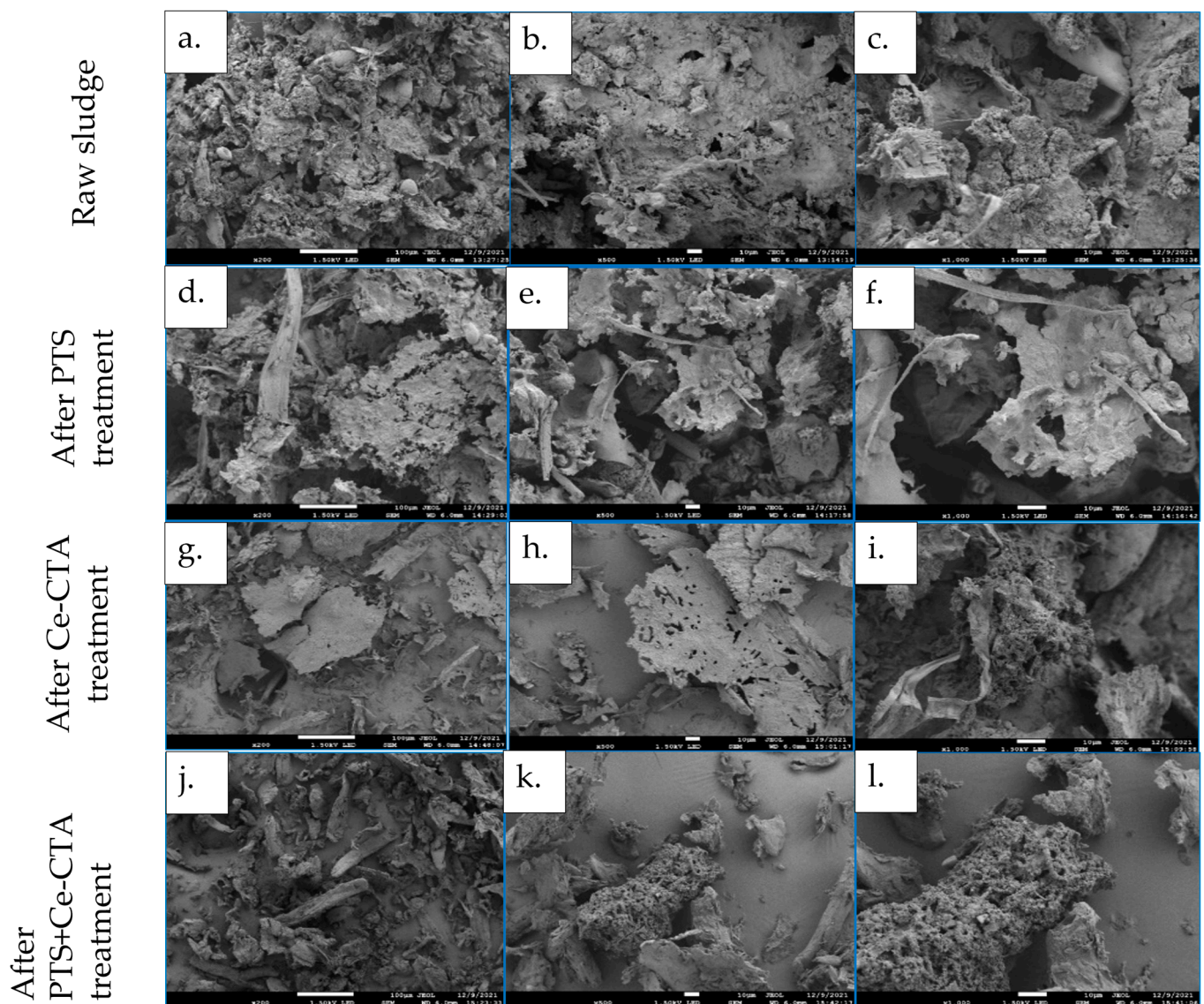


Figure 2. SEM images of sludge materials before and after treatment: (a–c) for raw sludge, (d–f) for sludge after PTS treatment, (g–i) for sludge after Ce-CTA treatment, and (j–l) for sludge after PTS+Ce-CTA treatment.

3.2. Sludge Dewaterability Check after Coagulation–Flocculation

The most important factor in sludge dewatering at the micro level is EPS. An abundance of highly hydrophilic oxygen-containing functional groups such as $-\text{COO}-$ and $-\text{CONH}-$ in sludge EPS leads to the formation of a hydrated biofilm on the surface of the sludge, which has a higher affinity for water. This surface isolates the particles in a steady state, which plays a considerable role in sludge dewaterability [38]. As a result, the EPS distribution and various compositions of LB-EPS and TB-EPS conditioned by different coagulant–flocculant combinations were studied further.

Figure 3 shows the EPS fractions in sludge samples and higher EPS contents were found after treatment. Newly prepared PTS solution was used and its coagulation efficiency evaluated with or without Ce-CTA addition. As we can see, the EPS content of sludge was affected a lot by coagulation–flocculation. At pH 3 and 6 EPS fractions rapidly increased using PTS and a moderate increase was seen for addition of only Ce-CTA. However, the combined PTS/Ce-CTA treatment showed the highest EPS concentration at pH 3. Most of the EPS increase is caused by sludge’s structural destruction and releasing of trapped water from the sludge. It may also enhance the sludge floc strength, which improves the sludge dewaterability.

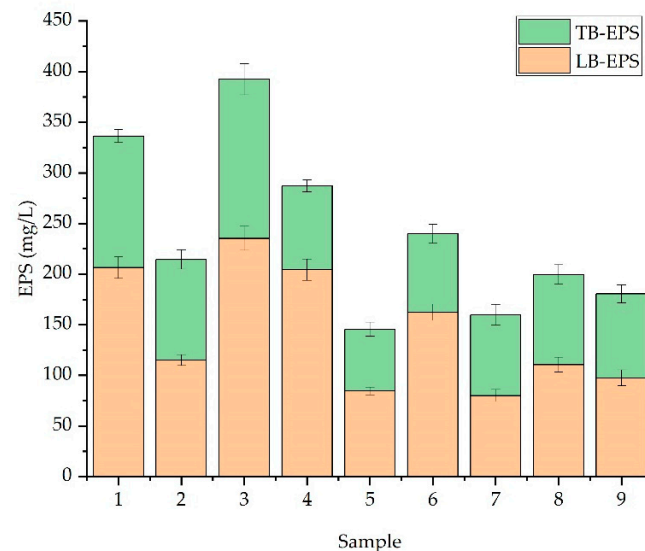


Figure 3. TB-EPS and LB-EPS conc. in sludge after coagulation–flocculation (batches 1, 2, 3 conducted at pH 3, batch 1 treated by PTS, batch 2 treated by Ce-CTA, and batch 3 by both PTS+Ce-CTA; batches 4, 5, 6 conducted at pH 6, batch 4 treated by PTS, batch 5 treated by Ce-CTA, and batch 6 by both PTS+Ce-CTA; batches 7, 8, 9 conducted at pH 9, batch 7 treated by PTS, batch 8 treated by Ce-CTA, and batch 9 by both PTS+Ce-CTA).

At pH 3, the EPS content increased to 340 mg/L when PTS was added for coagulation. EPS showed a value of 390 mg/L after PTS+Ce-CTA treatment, whereas it was 210 mg/L for Ce-CTA only. When the pH was 6, the EPS content was 270 mg/L for PTS treatment only and it decreased to 240 mg/L with combined treatment of PTS+Ce-CTA. For pH 9, the values of EPS content were lower compared to other pHs, but Ce-CTA showed the highest concentration of 190 mg/L. Generally, the sludge flocs cracking significantly enhances the organic content and EPS at different pH levels, which might be considered a reason for sludge dewaterability. These results suggested that the sludge matrix was broken by coagulants–flocculants and organic content released mostly from LB-EPS. We also assume that PTS mainly reduced the interfacial tension of sludge and solubilized the EPS leading to a higher concentration of EPS after treatment [39].

Studies have shown that sludge filterability is strongly dependent on the properties of the soluble EPS fraction, and the high protein content in this fraction has always been detrimental to filtration (Zhang et al., 2017). Furthermore, the subsequent sludge treatment

and disposal would be impacted by pH variations. Organic matter (e.g., protein-like) has been shown to undergo significant structural changes when subjected to acid treatment, which has been linked to the dissolution of EPS and cations (e.g., Ca^{2+} , Mg^{2+} , Al^{3+} , and Fe^{3+}) [4].

To increase sludge dewaterability, anaerobic digestion is used, which has high-performance and is energy efficient. Anaerobically digested sludge was evaluated in this study and sludge dewaterability can be improved by using a short-term digestion process at a suitable temperature as well. Combination of other treatment procedures such as acidification may improve the dewaterability of sludge. As tyrosine and tryptophan (protein-like compounds) in the EPS altered, the sludge's dewaterability improved initially but eventually deteriorated as a result. A combination of anaerobic digestion and acidification with organic content and flocculation was responsible for higher EPS content. The coagulant–flocculant dosage might be another reason for varied EPS content after treatment, so further investigation is required in future to check the dosage effect [40–42].

3.3. Heavy Metals Concentration before and after Treatment

Figure 4 shows the heavy metal concentration in the sludge supernatant. In total six heavy metals, Zn, Cr, Cu, Pb, Cd, and Fe, were considered here, and the extracted amount checked after coagulation–flocculation at different pHs. At pH 3 these metals were massively released into the supernatant after coagulation–flocculation. Some amount of Fe and Zn were found in sludge supernatant at neutral pH (6–7) after PTS treatment, but other metals were not extracted at this pH. Finally, at pH 9, no metals were found in the supernatant. Generally, because of their nonbiodegradability, heavy metals can be removed by changing their existence mode and transforming their speciation. pH affects the mobility of the heavy metals and generally, at lower pH, metals are released from sludge. In this study, the releasing rate $\text{Pb(II)} > \text{Cd(II)} > \text{Ni(II)}$ was obtained, which is consistent with the results by Król, Mizerna, and Bożym [43]. If we consider the Ce-CTA effect on heavy metals, then there is an exciting result at pH 6, where we found fewer heavy metals. Ce-CTA contains hydroxyl functional groups and showed a better adsorption quality as well, but pH affects the adsorption capacity of cellulose, so we did not find lower metal content at pH 9 [44]. Furthermore, inorganic materials as well as organics may enhance catalytic behavior, so after coagulation–flocculation, treated sludge materials could be used for catalyst preparation [45].

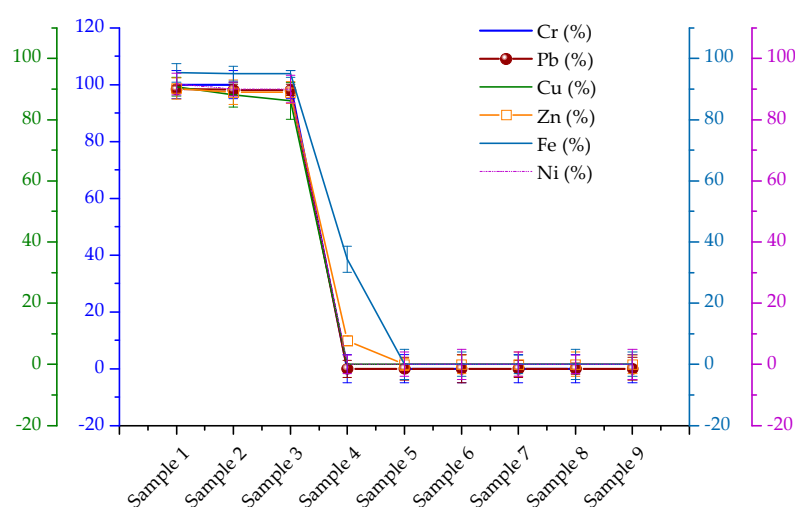


Figure 4. Metal concentration in sludge supernatant after coagulation–flocculation (samples 1, 2, 3 run at pH 3, sample 1 treated by PTS, sample 2 treated by Ce-CTA, and sample 3 by both PTS+Ce-CTA; samples 4, 5, 6 run at pH 6, sample 4 treated by PTS, sample 5 treated by Ce-CTA, and sample 6 by both PTS+Ce-CTA; samples 7, 8, 9 run at pH 9, sample 7 treated by PTS, sample 8 treated by Ce-CTA, and sample 9 by both PTS+Ce-CTA).

3.4. Nutrient Content after PTS and Ce-CTA Treatment

This research also analyzed the phosphorus recovery from the sludge during PTS, Ce-CTA, and combined PTS+Ce-CTA treatment. Three different pHs (3, 6, and 9) were considered to determine the phosphorus content in liquid phase after coagulation–flocculation. Anaerobically digested sludge that contains plenty of iron (Fe) and organic matter with other cations can interfere the P-dissolution [46]. In Figure 5, we can see that the highest rate of phosphorus recovery happened at pH 3 where only a minor difference was seen between PTS, Ce-CTA, and PTS+Ce-CTA treatments. PTS, Ce-CTA, and PTS+Ce-CTA extracted more than 95% of the total phosphorus at pH 3 after coagulation–flocculation, while PTS and PTS+Ce-CTA extracted about 80% of the total phosphorus at pH 9. In sludge supernatant, Ce-CTA extraction of phosphorus at pH 6 (nearly 70%) was not promising, but PTS and PTS+Ce-CTA showed >80% extraction in the sludge supernatant. If we only consider how acidification or alkalization caused phosphorus leaching in sludge, we can see that various researchers have explained it in various ways. According to Vardanyan et al. [47], at pH 3, phosphorus leaching efficiency was 76% and P-dissolution efficiencies reached peak at pH 2 (60% to 92%) from dewatered digested sludges. Carliell-Marquet et al. [48] studied the precipitation of phosphorus with Fe (III)-salts but could not fully explain the mechanisms. According to that study, Fe (III)-hydroxide precipitates and Fe (III)-hydroxy phosphate complexes were found as the most common forms of phosphorus and iron in activated sludge. Additionally, P extraction as magnesium aluminum phosphate was found to be greater in alkaline supernatant compared to acidic conditions [49].

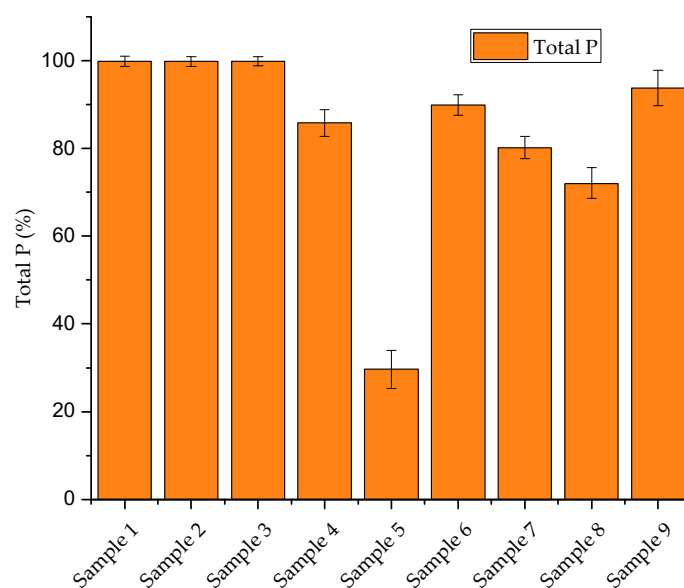


Figure 5. Total phosphorus conc. in sludge supernatant after coagulation–flocculation (samples 1, 2, 3 run at pH 3, sample 1 treated by PTS, sample 2 treated by Ce-CTA, and sample 3 by both PTS+Ce-CTA; samples 4, 5, 6 run at pH 6, sample 4 treated by PTS, sample 5 treated by Ce-CTA, and sample 6 by both PTS+Ce-CTA; samples 7, 8, 9 run at pH 9, sample 7 treated by PTS, sample 8 treated by Ce-CTA, and sample 9 by both PTS+Ce-CTA).

Orthophosphate and nitrate contents were also assessed from sludge supernatant by IC in Figure 5 and Table 1. Phosphorus exists as chemically bound, organically bound in sludge, and more than 80% of the P is dissolved by changing pH or acidification. Inorganic ortho-phosphate was detected in the samples with lower pH (at 3) but at neutral and alkaline pH supernatant phosphates were not present.

Table 1. Phosphate and nitrate conc. in sludge supernatant after coagulation–flocculation (Samples 1, 2, 3 conducted coagulation test at pH 3 by PTS, Ce-CTAs and PTS+Ce-CTA; Samples 4, 5, 6 analysis at pH 6 by PTS, Ce-CTA, and PTS+Ce-CTA; Samples 7, 8, 9 assessed at pH 9 by PTS, Ce-CTA, and PTS+Ce-CTA).

Sample No.	Nitrate (ppm)	Phosphate (ppm)
Sample 1 (pH 3)	5.063 ± 0.5	15 ± 2.05
Sample 2 (pH 3)	5.063 ± 0.43	9 ± 1.01
Sample 3 (pH 3)	5.314 ± 0.32	18 ± 3.05
Sample 4 (pH 6)	5.328 ± 0.31	×
Sample 5 (pH 6)	×	×
Sample 6 (pH 6)	×	×
Sample 7 (pH 9)	5.031 ± 0.51	×
Sample 8 (pH 9)	×	×
Sample 9 (pH 9)	×	×

Although XRD clearly detected AlPO_4 , other P-containing phases may also be present, given that a concomitant release of Al always accompanies the extraction of P, Ca, and Fe in both sequential fractionation and independent extraction.

Nitrate concentration after sludge treatment was quite low in the supernatant most probably due to adsorption of nitrate on the sludge materials. It is also commonly known that the high binding of P in sewage sludge to iron or aluminum phosphate after chemical precipitation restricts recovery of phosphorus from the waste product. However, at low pH phosphorus reacts with Al, Fe, and as an initial step in P recovery, it is dispersed into the liquid phase from sewage or anaerobic sludge. Precipitation with Na_2S or NaOH can be used to remove ions and heavy metals from the liquid phase. Finally, P can be recovered as struvite or calcium phosphate through crystallization and nitrate can be recovered and used as nutrient in fertilizer [47,48,50]. The concentrations of nutrients in the sludge supernatant varied when tested by PTS, Ce-CTA, and PTS+Ce-CTA at various pH ranges. After the coagulation–flocculation process, the nutrients (phosphorus and nitrate) recovered could be recycled and utilized as resources.

3.5. Photocatalytic Activity of Sludge after Coagulation–Flocculation

After PTS treatment, sludge materials before and after pyrolysis were tested as photocatalysts to degrade tetracycline. The photocatalytic activity of sludge after coagulation–flocculation and after pyrolysis was tested and found to be more effective under UV light than visible light.

The photocatalytic activities of raw sludge, and pyrolyzed sludge as the modified one, were measured through tetracycline under visible and UV light as there was not any significant result under visible light. So, UV light was used for TeC degradation for further studies in Figure 6. As shown in Figure 6a, the pyrolyzed sludge degraded 80% of tetracycline after 220 min, whereas only 55% was degraded by dried sludge. Experiments with different pHs showed highest degradation efficiency for pyrolyzed sludge at pH 4. Furthermore, Figure 6c shows that the concentration of tetracycline decreased significantly more efficiently under UV light compared to the absence of light, proving its potential as a low cost photocatalyst for further applications.

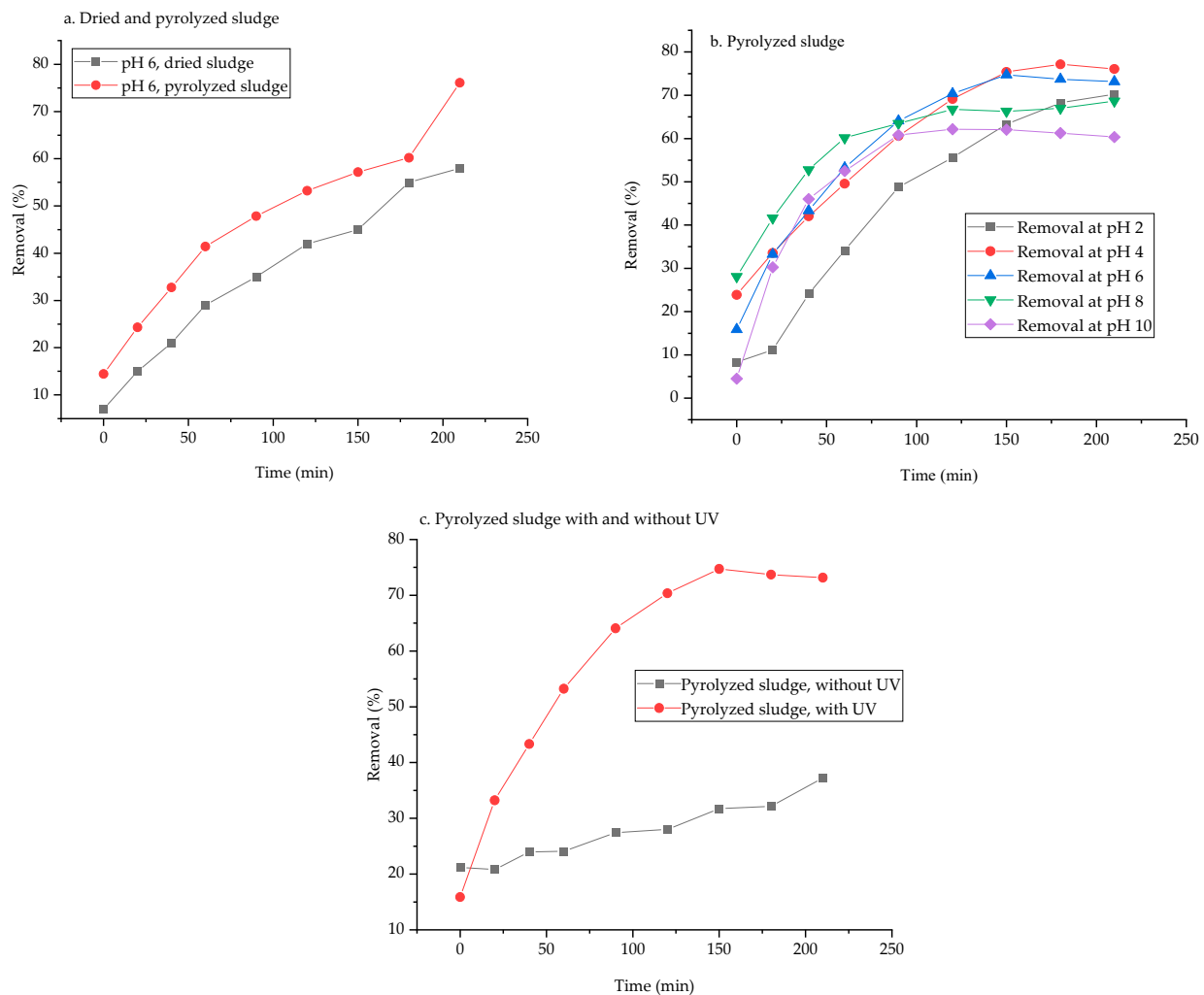


Figure 6. Photocatalytic activity of sludge before and after pyrolysis (TeC conc. 20 ppm, dosage 0.5 g/L): (a) TeC degradation by dried and pyrolyzed sludge under UV at pH 6, (b) TeC degradation by pyrolyzed sludge at different pH, and (c) TeC degradation by pyrolyzed sludge with or without UV light at pH 4.

4. Conclusions and Future Perspective

The coagulation–flocculation process using organic coagulants and inorganic flocculants (natural and cellulose-based) was investigated in this study for anaerobically digested sludge treatment. Sludge dewaterability was assessed after the treatment and higher protein and polysaccharide concentrations were found at pH 3 compared to neutral and alkaline samples. At pH 3, the EPS content increased to 340 mg/L with PTS treatment and to 390 mg/L after PTS+Ce-CTA treatment. When the pH was 6, the EPS content was 270 mg/L for PTS treatment only, and it decreased to 240 mg/L with combined treatment of PTS+Ce-CTA. Phosphate showed higher concentration (15 ppm) in sludge supernatant at acidic pH after PTS treatment and it increased to 18 ppm after PTS+Ce-CTA treatment. Most promising from this investigation was to investigate the PTS treated sludge as a photocatalyst and create a future application of sludge materials after coagulation–flocculation. Especially, Ti-containing pyrolyzed sludge effectively degraded tetracycline under UV radiation. In summary, the coagulation–flocculation treatment of sludge improves SVI and develops the possibility to recover nutrients from sludge supernatant. Recovery of coagulants–flocculants should also be considered in order to enhance the circular economy of sludge materials. Moreover, Ti-coagulants have the most significant potential to replace

traditional coagulants since sludge can be recycled as catalysts as well as in other areas, e.g., building materials, carbon-based materials, and biochar.

Supplementary Materials: The following supporting information can be downloaded at: <https://www.mdpi.com/article/10.3390/resources12020017/s1>, Figure S1: FTIR analysis of PTS with different ratios: (a) PTS 1:1 ratio, (b) PTS 1:2 ratio, and (c) PTS 1:3 ratio. Figure S2: FTIR analysis of PTS with different ratios: (a) PTS 1:4 ratio, (b) PTS 1:5 ratio. Figure S3: FTIR analysis of synthesized Ce-CTA material. Figure S4: XRD analysis of sludge materials after coagulation–flocculation at pH 3: (a) Sample 1—raw sludge, (b) Sample 2 with PTS only, (c) Sample 3 with Ce-CTA, and (d) Sample 4 with PTS+Ce-CTA. Figure S5: XRD analysis of sludge materials after coagulation–flocculation at pH 6: (a) Sample 5 with PTS only, (b) Sample 6 with Ce-CTA, and (c) Sample 7 with PTS+Ce-CTA. Figure S6: XRD analysis of sludge materials after coagulation–flocculation at pH 9: (a) Sample 8 with PTS only, (b) Sample 9 with Ce-CTA, and (c) Sample 10 with PTS+Ce-CTA.

Author Contributions: J.R.: Conceptualization, methodology, formal analysis, investigation, and writing—original draft. E.B.: Formal analysis, Investigation. E.R.: Writing—review and editing, supervision, project administration, and funding acquisition. All authors have read and agreed to the published version of the manuscript.

Funding: This research received no external funding.

Institutional Review Board Statement: Not applicable.

Informed Consent Statement: Not applicable.

Data Availability Statement: Not applicable.

Conflicts of Interest: Authors state that no conflict of interest or personal relationships could have appeared to influence the work presented in this research.

References

1. He, D.; Sun, M.; Bao, B.; Chen, J.; Luo, H.; Li, J. Rethinking the timing of flocculant addition during activated sludge dewatering. *J. Water Process Eng.* **2022**, *47*, 102744. [[CrossRef](#)]
2. Hyrycz, M.; Ochowiak, M.; Krupińska, A.; Włodarczak, S.; Matuszak, M. A review of flocculants as an efficient method for increasing the efficiency of municipal sludge dewatering: Mechanisms, performances, influencing factors and perspectives. *Sci. Total Environ.* **2022**, *820*, 153328. [[CrossRef](#)] [[PubMed](#)]
3. Cao, B.; Zhang, W.; Wang, Q.; Huang, Y.; Meng, C.; Wang, D. Wastewater sludge dewaterability enhancement using hydroxyl aluminum conditioning: Role of aluminum speciation. *Water Res.* **2016**, *105*, 615–624. [[CrossRef](#)] [[PubMed](#)]
4. Zhang, W.; Chen, Z.; Cao, B.; Du, Y.; Wang, C.; Wang, D.; Ma, T.; Xia, H. Improvement of wastewater sludge dewatering performance using titanium salt coagulants (TSCs) in combination with magnetic nano-particles: Significance of titanium speciation. *Water Res.* **2017**, *110*, 102–111. [[CrossRef](#)]
5. Liang, J.; Zhang, S.; Huang, J.; Huang, S.; Zheng, L.; Sun, S.; Zhong, Z.; Zhang, X.; Yu, X. Comprehensive insights into the inorganic coagulants on sludge dewatering: Comparing aluminium and iron salts. *J. Chem. Technol. Biotechnol.* **2019**, *94*, 1534–1550. [[CrossRef](#)]
6. Golbabaee Kootenaee, F.; Mehrdadi, N.; Nabi Bidhendi, G.; Amini Rad, H.; Hasanlou, H.; Mahmoudnia, A. Improvement of Sludge Dewatering by Ultrasonic Pretreatment. *Int. J. Environ. Res.* **2022**, *16*, 50. [[CrossRef](#)]
7. Ling, X.; Cai, A.; Chen, M.; Sun, H.; Xu, S.; Huang, Z.; Li, X.; Deng, J. A comparison of oxidation and re-flocculation behaviors of Fe²⁺/PAA and Fe²⁺/H₂O₂ treatments for enhancing sludge dewatering: A mechanism study. *Sci. Total Environ.* **2022**, *847*, 157690. [[CrossRef](#)]
8. Ling, X.; Deng, J.; Ye, C.; Cai, A.; Ruan, S.; Chen, M.; Li, X. Fe(II)-activated sodium percarbonate for improving sludge dewaterability: Experimental and theoretical investigation combined with the evaluation of subsequent utilization. *Sci. Total Environ.* **2021**, *799*, 149382. [[CrossRef](#)] [[PubMed](#)]
9. Wu, B.; Dai, X.; Chai, X. Critical review on dewatering of sewage sludge: Influential mechanism, conditioning technologies and implications to sludge re-utilizations. *Water Res.* **2020**, *180*, 115912. [[CrossRef](#)]
10. Ruiz-Hernando, M.; Simón, F.X.; Labanda, J.; Llorens, J. Effect of ultrasound, thermal and alkali treatments on the rheological profile and water distribution of waste activated sludge. *Chem. Eng. J.* **2014**, *255*, 14–22. [[CrossRef](#)]
11. Mowla, D.; Tran, H.N.; Allen, D.G. A review of the properties of biosludge and its relevance to enhanced dewatering processes. *Biomass Bioenergy* **2013**, *58*, 365–378. [[CrossRef](#)]
12. Chen, Z.; Zhang, W.; Wang, D.; Ma, T.; Bai, R. Enhancement of activated sludge dewatering performance by combined composite enzymatic lysis and chemical re-flocculation with inorganic coagulants: Kinetics of enzymatic reaction and re-flocculation morphology. *Water Res.* **2015**, *83*, 367–376. [[CrossRef](#)] [[PubMed](#)]

13. Zhao, Y.-X.; Li, X.-Y. Polymerized titanium salts for municipal wastewater preliminary treatment followed by further purification via crossflow filtration for water reuse. *Sep. Purif. Technol.* **2019**, *211*, 207–217. [[CrossRef](#)]
14. Gan, Y.; Li, J.; Zhang, L.; Wu, B.; Huang, W.; Li, H.; Zhang, S. Potential of titanium coagulants for water and wastewater treatment: Current status and future perspectives. *Chem. Eng. J.* **2021**, *406*, 126837. [[CrossRef](#)]
15. Lee, B.C.; Kim, S.; Shon, H.K.; Vigneswaran, S.; Kim, S.D.; Cho, J.; Kim, I.S.; Choi, K.H.; Kim, J.B.; Park, H.J.; et al. Aquatic toxicity evaluation of TiO₂ nanoparticle produced from sludge of TiCl₄ flocculation of wastewater and seawater. *J. Nanoparticle Res.* **2009**, *11*, 2087–2096. [[CrossRef](#)]
16. Bondy, S.C. Low levels of aluminum can lead to behavioral and morphological changes associated with Alzheimer's disease and age-related neurodegeneration. *Neurotoxicology* **2016**, *52*, 222–229. [[CrossRef](#)] [[PubMed](#)]
17. Niu, M.; Zhang, W.; Wang, D.; Chen, Y.; Chen, R. Correlation of physicochemical properties and sludge dewaterability under chemical conditioning using inorganic coagulants. *Bioresour. Technol.* **2013**, *144*, 337–343. [[CrossRef](#)]
18. Yang, R.; Li, H.; Huang, M.; Yang, H.; Li, A. A review on chitosan-based flocculants and their applications in water treatment. *Water Res.* **2016**. [[CrossRef](#)]
19. Pellizzer, L. Synthesis of Cellulose-Based Flocculants and Performance Tests. Ph.D. Thesis, Universidade de Coimbra, Coimbra, Portugal, 2016; p. 113.
20. Ida, S.; Eva, T. Removal of heavy metals during primary treatment of municipal wastewater and possibilities of enhanced removal: A review. *Water* **2021**, *13*, 1121. [[CrossRef](#)]
21. Ghodsi, V.; Sarathy, S.R.; Walton, J.R.; Watson, I.; Elbeshbishy, E.; Santoro, D. Enhancing sludge dewaterability and phosphate removal through a novel chemical dosing strategy using ferric chloride and hydrogen peroxide. *Water Environ. Res.* **2021**, *93*, 232–240. [[CrossRef](#)]
22. Chu, Y.-B.; Li, M.; Liu, J.-W.; Xu, W.; Cheng, S.-H.; Zhao, H.-Z. Molecular insights into the mechanism and the efficiency-structure relationship of phosphorus removal by coagulation. *Water Res.* **2018**, *147*, 195–203. [[CrossRef](#)] [[PubMed](#)]
23. Melia, P.M.; Cundy, A.B.; Sohi, S.P.; Hooda, P.S.; Busquets, R. Trends in the recovery of phosphorus in bioavailable forms from wastewater. *Chemosphere* **2017**, *186*, 381–395. [[CrossRef](#)] [[PubMed](#)]
24. Wei, H.; Ren, J.; Li, A.; Yang, H. Sludge dewaterability of a starch-based flocculant and its combined usage with ferric chloride. *Chem. Eng. J.* **2018**, *349*, 737–747. [[CrossRef](#)]
25. APHA/AWWA/WEF. *Standard Methods for the Examination of Water and Wastewater*; American Public Health Association: Washington, DC, USA, 2012; Volume 541, ISBN 9780875532356.
26. Ding, T.; Ding, M.; Lu, C.; Cui, J.; Shen, K.; Xu, H. Dewatering of drinking water treatment sludge using the Fenton-like process induced by electro-osmosis. *Chem. Eng. J.* **2016**, *293*, 207–215. [[CrossRef](#)]
27. Zhou, J.; Zheng, G.; Zhang, X.; Zhou, L. Influences of extracellular polymeric substances on the dewaterability of sewage sludge during bioleaching. *PLoS ONE* **2014**, *9*, e102688. [[CrossRef](#)]
28. Frølund, B.; Palmgren, R.; Keiding, K.; Nielsen, P.H. Extraction of extracellular polymers from activated sludge using a cation exchange resin. *Water Res.* **1996**, *30*, 1749–1758. [[CrossRef](#)]
29. Xu, Y.; Hu, H.; Liu, J.; Luo, J.; Qian, G.; Wang, A. pH dependent phosphorus release from waste activated sludge: Contributions of phosphorus speciation. *Chem. Eng. J.* **2015**, *267*, 260–265. [[CrossRef](#)]
30. Rumky, J.; Visigalli, S.; Turolla, A.; Gelmi, E.; Necibi, C.; Gronchi, P.; Sillanpää, M.; Canziani, R. Electro-dewatering treatment of sludge: Assessment of the influence on relevant indicators for disposal in agriculture. *J. Environ. Manage.* **2020**, *268*, 110689. [[CrossRef](#)]
31. Huang, X.; Gao, B.; Wang, Y.; Yue, Q.; Li, Q.; Zhang, Y. Coagulation performance and flocs properties of a new composite coagulant: Poly titanium–silicate–sulfate. *Chem. Eng. J.* **2014**, *245*, 173–179. [[CrossRef](#)]
32. Ejimofor, M.I.; Ezemagu, I.G.; Menkiti, M.C. Physicochemical, Instrumental and thermal characterization of the post coagulation sludge from paint industrial wastewater treatment. *S. Afr. J. Chem. Eng.* **2021**, *37*, 150–160. [[CrossRef](#)]
33. Al-Amin, M.; Chandra Dey, S.; Rashid, T.U.; Ashaduzzaman, M.; Shamsuddin, S.M. Solar Assisted Photocatalytic Degradation of Reactive Azo Dyes in Presence of Anatase Titanium Dioxide. *Int. J. Latest Res. Eng. Technol.* **2016**, *2*, 14–21.
34. Kiefer, J.; Strk, A.; Kiefer, A.L.; Glade, H. Infrared spectroscopic analysis of the inorganic deposits from water in domestic and technical heat exchangers. *Energies* **2018**, *11*, 798. [[CrossRef](#)]
35. Liberatore, M.W.; Peterson, B.N.; Nottoli, T.; McCulloch, J.M.; Jinkerson, R.E.; Boyle, N.R.; Posewitz, M.C. Effectiveness of cationically modified cellulose polymers for dewatering algae. *Sep. Sci. Technol.* **2016**, *51*, 892–898. [[CrossRef](#)]
36. Abderrahim, B.; Abderrahman, E.; Mohamed, A.; Fatima, T.; Abdesselam, T.; Krim, O. Kinetic Thermal Degradation of Cellulose, Polybutylene Succinate and a Green Composite: Comparative Study. *World J. Environ. Eng.* **2015**, *3*, 95–110. [[CrossRef](#)]
37. Uysal, A.; Boyacioglu, E. Evaluation of the performance of titanium and zirconium salts as coagulants in industrial wastewater treatment: Pollutant removal, sludge production, and sludge characteristics. *Appl. Water Sci.* **2021**, *11*, 78. [[CrossRef](#)]
38. Masihi, H.; Badalians Gholikandi, G. Using acidic-modified bentonite for anaerobically digested sludge conditioning and dewatering. *Chemosphere* **2020**, *241*, 125096. [[CrossRef](#)]
39. Dong, Y.; Gu, M.; Yuan, H.; Zhu, N. Insights into the enhancement of waste activated sludge dewaterability using sodium dichloroisocyanurate and dodecyl dimethyl ammonium chloride: Performance, mechanism, and implication. *Sci. Total Environ.* **2021**, *778*, 146302. [[CrossRef](#)]

40. Lan, B.; Jin, R.; Liu, G.; Dong, B.; Zhou, J.; Xing, D. Improving waste activated sludge dewaterability with sodium periodate pre-oxidation on extracellular polymeric substances. *Water Environ. Res.* **2021**, *93*, 1680–1689. [[CrossRef](#)]
41. Zhang, S.; Liang, J.; Huang, J.; Huang, S.; Zheng, L.; Sun, S.; Zhong, Z.; Zhang, X.; Yu, X.; Guan, Z. Analysis of the relationship of extracellular polymeric substances to the dewaterability and rheological properties of sludge treated by acidification and anaerobic mesophilic digestion. *J. Hazard. Mater.* **2019**, *369*, 31–39. [[CrossRef](#)]
42. Houghton, J.I.; Stephenson, T. Effect of influent organic content on digested sludge extracellular polymer content and dewaterability. *Water Res.* **2002**, *36*, 3620–3628. [[CrossRef](#)]
43. Król, A.; Mizerna, K.; Bożym, M. An assessment of pH-dependent release and mobility of heavy metals from metallurgical slag. *J. Hazard. Mater.* **2020**, *384*, 121502. [[CrossRef](#)]
44. Jamshaid, A.; Hamid, A.; Muhammad, N.; Naseer, A.; Ghauri, M.; Iqbal, J.; Rafiq, S.; Shah, N.S. Cellulose-based Materials for the Removal of Heavy Metals from Wastewater—An Overview. *ChemBioEng Rev.* **2017**, *4*, 240–256. [[CrossRef](#)]
45. Chen, X.; Fu, L.; Yu, Y.; Wu, C.; Li, M.; Jin, X.; Yang, J.; Wang, P.; Chen, Y. Recent Development in Sludge Biochar-Based Catalysts for Advanced Oxidation Processes of Wastewater. *Catalysts* **2021**, *11*, 1275. [[CrossRef](#)]
46. Monea, M.C.; Löhr, D.K.; Meyer, C.; Preyl, V.; Xiao, J.; Steinmetz, H.; Schönberger, H.; Drenkova-Tuhtan, A. Comparing the leaching behavior of phosphorus, aluminum and iron from post-precipitated tertiary sludge and anaerobically digested sewage sludge aiming at phosphorus recovery. *J. Clean. Prod.* **2020**, *247*, 119129. [[CrossRef](#)]
47. Vardanyan, A.; Kafa, N.; Konstantinidis, V.; Shin, S.G.; Vyrides, I. Phosphorus dissolution from dewatered anaerobic sludge: Effect of pHs, microorganisms, and sequential extraction. *Bioresour. Technol.* **2018**, *249*, 464–472. [[CrossRef](#)] [[PubMed](#)]
48. Carliell-Marquet, C.; Smith, J.; Oikonomidis, I.; Wheatley, A. Inorganic profiles of chemical phosphorus removal sludge. *Proc. Inst. Civ. Eng.-Water Manag.* **2010**, *163*, 65–77. [[CrossRef](#)]
49. Xu, D.; Zhong, C.; Yin, K.; Peng, S.; Zhu, T.; Cheng, G. Alkaline solubilization of excess mixed sludge and the recovery of released phosphorus as magnesium ammonium phosphate. *Bioresour. Technol.* **2018**, *249*, 783–790. [[CrossRef](#)] [[PubMed](#)]
50. Wilfert, P.; Mandalidis, A.; Dugulan, A.I.; Goubitz, K.; Korving, L.; Temmink, H.; Witkamp, G.J.; Van Loosdrecht, M.C.M. Vivianite as an important iron phosphate precipitate in sewage treatment plants. *Water Res.* **2016**, *104*, 449–460. [[CrossRef](#)]

Disclaimer/Publisher’s Note: The statements, opinions and data contained in all publications are solely those of the individual author(s) and contributor(s) and not of MDPI and/or the editor(s). MDPI and/or the editor(s) disclaim responsibility for any injury to people or property resulting from any ideas, methods, instructions or products referred to in the content.